INFLATABLE SPACE SHIELD STRUCTURE FOR SPACE HABITATION MODULE

Ji-Hun Cha¹

Department of Aerospace Engineering, Chosun University, 309 Pilmun-daero, Dong-gu, Gwangju, Republic of Korea

The Whipple shield is used in spacecraft as an outer wall structure to protect against micrometeoroids. By increasing the stand-off distance of the Whipple shield and using a multilayered shield structure, it is possible to increase bulletproof performance against micrometeoroids. Due to payload diameter limitations, the Whipple shield's stand-off distance cannot be significantly increased. Increasing the stand-off distance of the Whipple shield reduces the volume inside the spacecraft. To solve this problem, an origami structure in which a multilayer shield expands in a radial direction has been proposed. PE/Epoxy composites have been proposed to realize origami structures. When the PE/Epoxy composites were bent, the resistance to the low-Earth orbit space environment was evaluated and compared with that of the plane PE/Epoxy composites. In order to increase the resistance to the space environment, a method of secondary curing of Kapton and bulletproof fibers together in the flexible part has been proposed. Hypervelocity impact tests were conducted to improve and verify the performance of the proposed inflatable structure. The radiant heat shielding performance of the proposed multilayer structure of ceramic fibers and flexible composites and multi-layer insulation (MLI) was compared, and it was confirmed that the radiant heat shielding performance was comparable to that of MLI. The geometry of the proposed inflatable origami structure was analyzed and the folding pattern was determined. The proposed inflatable origami structure confirmed the diameter reduction effect and improved bulletproof performance compared to the conventional Whipple shielding structure.

I. Nomenclature

MMOD = inflatable origami multi-shock shield structure
 IMSS = Inflatable origami multi-shock shield structure

NPEC = Nextel/PE/Epoxy composite

PE = Ultra-high-molecular-weight polyethylene fiber

PEC = PE/Epoxy composite LEO = Low earth orbit HVI = Hypervelocity impact

¹ Assistant Professor, Department of Aerospace Engineering; space composites@chosun.ac.kr

II. Introduction

With the substantial increase of space activities, the space environment has deteriorated sharply. In particular, the large-scale development of the LEO constellation satellite will increase the probability of explosive growth in the number of the orbital debris [1].

To protect the spacecraft from space debris (or micrometeoroids), the Whipple shield is used as the outer wall structure of the spacecraft. Increasing the stand-off distance of the Whipple shield and making it a multi-layered shield structure can increase bulletproof performance in high-velocity collisions, but the stand-off distance cannot be greatly increased due to the limitation of the payload diameter. Stand-off distance cannot be significantly increased due to payload diameter limitations. Also, as the stand-off distance is increased, the space inside the spacecraft becomes smaller. Therefore, if an inflatable structure is applied to the Whipple shield, a multi-layered shield structure can be realized by increasing the stand-off distance, and at the same time, the space inside the spacecraft can be greatly used. However, currently no research related to the inflatable space shield has been reported. In order to solve these multifield problems, it is proposed to apply an expandable structure (stand-off distance increase) for the purpose of imparting multifunctionality of microplanetary shielding to materials and structures effective for shielding cosmic radiation [2-3].

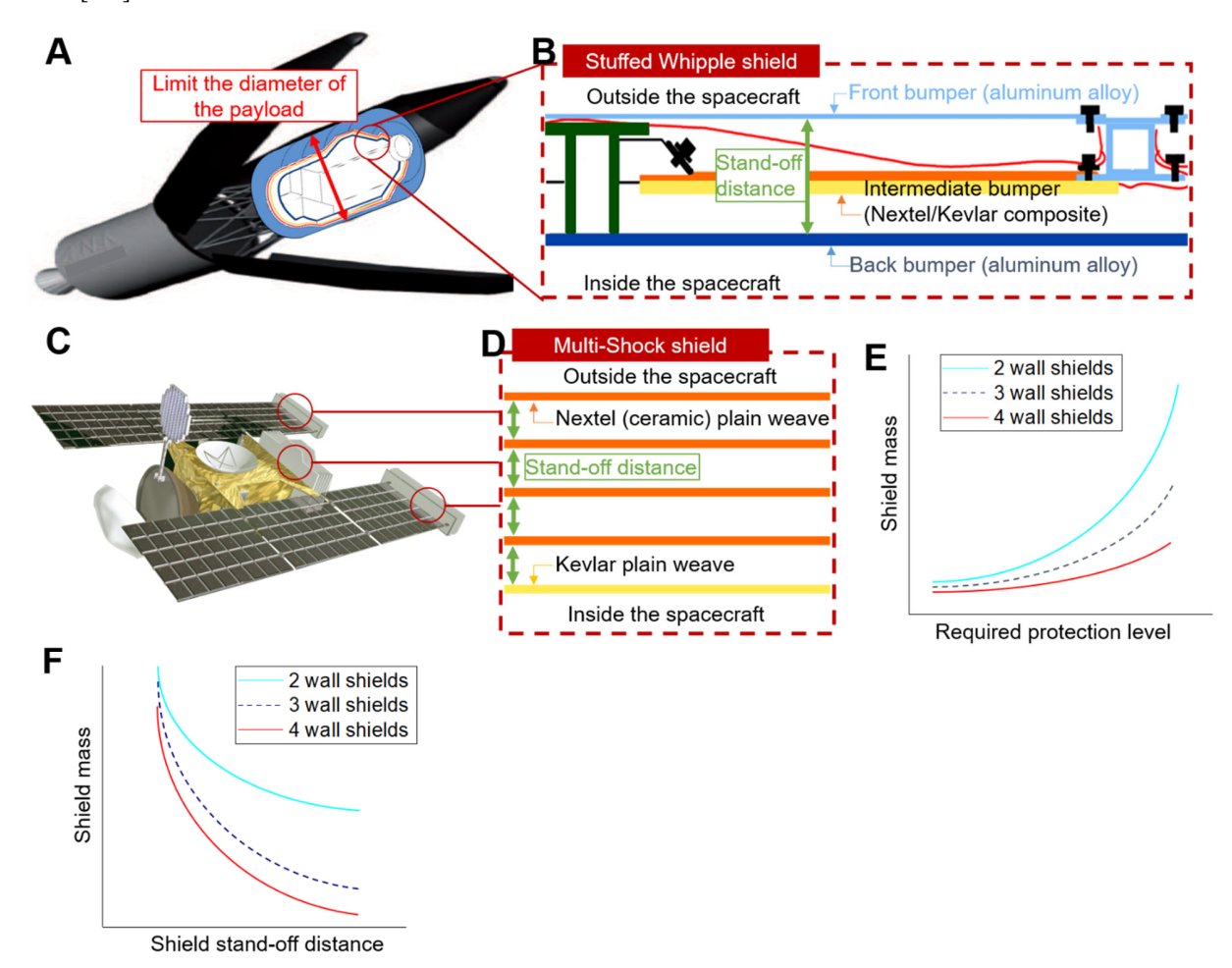


Fig. 1 Research background. (A) Space debris and micrometeorite in earth orbit. (B) Limit the diameter of the payload. (C) Whipple shield structure for space debris shielding. (D) The shielding mass reduction effect of multi-layer structure and stand-off distance.

Ultra-high-molecular-weight-polyethylene fiber (PE) is used as a bulletproof material. UHMWPE exhibits less plastic deformation due to repeated bending than carbon fiber or glass fiber. In addition, there are cases where UHMWPE is used as a tether for actual spacecraft. Therefore, PE/epoxy composites has been proposed as a material for the inflatable structure [4].

According to the dimensions of the proposed inflatable origami shield structure (IMSS), the gap and number of bumpers after inflation can be set. Therefore, the proposed structure can be optimally designed when the number and spacing of bumpers are determined from the results of HVI. Although this study could not suggest effective bumper spacing and number of bumpers for HVI due to experimental limitations (ballistic size and velocity), the empirical model shown in this study can increase the radius after expansion by about 80% from the initial radius. Conventional Whipple shields require a secondary structure that does not help the shield much to connect the bumper. However, the proposed IMSS has almost no secondary structures that are not helpful for the shield. Therefore, almost all of the mass used in the bumper can contribute to the shield, leading to a lightweight effect. In addition, it has a flexible structure with a large thickness-to-length ratio, and in many parts, it can absorb more energy with flexible movement in HVI, similar to free constraints [5-8].

Although a lot of load is not required for deployment in outer space, a structure has been proposed through many trials and errors to reduce the pre-inflation volume while eliminating parts that require excessive force to reduce the energy required for deployment. The multi-shock shield concept has been proven to be bulletproof through various studies and was actually used in the comet probe stardust and Comet Nucleus Tour. However, the LEO spacecraft could not be applied due to the volume limitations of the payload diameter. Rather than making the bumper one thick layer, making it multi-layered allows the bumper to have a more flexible structure as the thickness-to-length ratio of the bumper decreases. A bumper without internal support will have a small length-to-thickness ratio, which has another advantage of absorbing more energy in a high-speed collision while having a flexible structure similar to the free-boundary condition in a high-speed collision. Various origami patterns for expanding the diameter have been implemented, and we paid attention to the waterbomb tessellation origami pattern among them. This configuration allows for radial expansion with one degree of freedom. The waterbomb-based shield structure forms an outer layer in the same direction as the fuselage, and has no parts connected to the fuselage except for the contact points at both ends of the fuselage. In other words, most of the elements that make up the bumper can contribute to the shield, which leads to a shielding and lightweight effect [9-12].

III. RESULTS

A. Design of inflatable origami space shield structure

The design of IMSS is inspired by inflatable wheel structures such as Lee et al. [1]. The transition from a paper model to an origami structure with rigid and flexible parts is designed by determining the basic length of the membrane gap (*I*), a design parameter. Given simple folding with two facets, the minimum *I* is twice the facet thickness for flat folding potential. However, thick membranes with high curvature induce significant resistive forces and energy accumulation. On the other hand, increasing *I* causes the whole structure to deviate from the desired shape. Previous studies have used the Euler-Bernoulli beam theory to select an appropriate spacing for this parameter. In other words, the gap leading to the circle was determined as the basic length. In addition, it was confirmed that the space environment resistance varies according to the curvature of the proposed PE/epoxy composite, and it was confirmed that excessive folding not only requires a lot of energy for unfolding, but also adversely affects the space environment resistance.

1) Design and geometry of an inflatable space shield structure: Achieving kinematic degrees of freedom is the next step in pattern design. The proposed design of the multilayer shield side creates a dependence between the pre-inflation length and the post-inflation length at each bumper, which is shown in Figures 2 (B) and (D). The multilayer shield structure consists of a rim part that makes the outer edge of the wheel of the shield, a shield hub that is combined with

the fuselage, and a spoke part that connects the rim part. The length of the rim part parallel to the side is the same for all bumpers, which is shown in green in Figure 2. The difference in the angle of inclination of the spoke part, which is a shield folded at an angle, and the length of the connecting part of the HUB allows it to expand wider while having the same length before and after expansion. The length of each part in the side design of the multi-layer shield under the geometrical conditions of the first-stage bumper and the second-stage bumper before and after expansion can be calculated as follows:

From Figure 2 (F),

$$(x_1 + d_1)^2 = (d_1 + d_2 - h)^2 + (x_1)^2$$
(1)

On the other hand, in order to maximize the diameter before deployment, the one-layer bumper spacing (h) is designed to use a thin space corresponding to the bumper thickness. However, for bumper inclusion, which will be explained later, h must be at least three times the thickness of the bumper. Therefore, h is determined by the thickness of the bumper to be applied. d_1 and d_2 can be determined for optimal performance in HVI. Bumper clearances of 50-100 mm were used on the TransHab and Comet Nucleus Tour in previous studies.

Solving the equation of Eq. (1),

$$x_1 = \frac{h^2 - 2h(d_1 + d_2) + d_2(2d_1 + d_2)}{2d_1} \tag{2}$$

If d_1 and d_2 are equal, x_1 can be simplified as.

$$x_1 = \frac{h^2 - 4hd_1 + 3d_1^2}{2d_1} \tag{3}$$

The length of each part in the side design of the multi-layer shield under geometrical conditions of the two-stage bumper and the three-stage bumper before and after expansion can be calculated as follows:

From Figure 2 (G),

$$(x_2 + d_1)^2 = (d_1 + d_2 + d_3 - 2h)^2 + (x_2)^2$$
(4)

$$x_2 = \frac{4h^2 - 4h(d_1 + d_2 + d_3) + (d_2 + d_3)(2d_1 + d_2 + d_3)}{2d_1}$$
(5)

If d_1 , d_2 , and d_3 are equal,

$$(x_n + d_1)^2 = (d_1 + \sum_{i=2}^{i=n+1} d_i - n \times h)^2 + (x_n)^2$$
(6)

$$x_n = \frac{n^2 h^2 - 2(n^2 + n)d_1 h + d_1^2 (n^2 + 2n)}{2d_2} \tag{7}$$

n is a factor that determines the number of bumpers, and x_{n-l} is the length of the section where the nth bumper requires slope shielding. The design rule to accommodate the thickness of facet and membrane was applied and calculated, but the value for l was approximated to be equal to 90 degree bending at any oblique bending angle, and as a result, l was eliminated from the equation. Depending on the inclination angle difference, the dimension for l is inaccurate, but l is very small compared to the overall length. Also, an imprecise dimension for l has no effect on the expansion mechanism, only a minor effect on the value of d.

Figure 2 (H) shows the graph calculated by Equation 7. Considering the thickness of the Nextel/PE/epoxy composite (less than 2 mm) and manufacturing tolerance, h=10 mm is determined and the graph is drawn. This is still

a very small value considering the spacecraft's diameter is about 4.5 m. From the graph, the maximum slope length increases as the number of bumpers and the bumper spacing increase. The length of a typical space module is about 7m (EAS ATV, Destiny, Columbus). Therefore, the maximum slope length (x_{n-1}) in a space module can be limited to about 3m or less. As shown in the graph, in order to realize a 10-layer bumper at a maximum slope length of 3m or less, it must be designed with an interval of 80mm or less. If the TransHab shield (d=100mm, n=5) is implemented as the IMSS in this study, the maximum slope length is 1m and the spacing can be made 100mm. Similarly, if the Comet Nucleus Tour shield (d=50mm, n=5) is implemented as IMSS, it can be implemented with a maximum slope length of about 0.4m to realize 50mm spacing between 5 bumpers. At this time, 5 bumpers occupy only 50mm of space in the diametric direction, and can save 90% of the diametrical volume compared to the space of 500mm. Of course, more diametric volume can be saved if d is further increased for better performance.

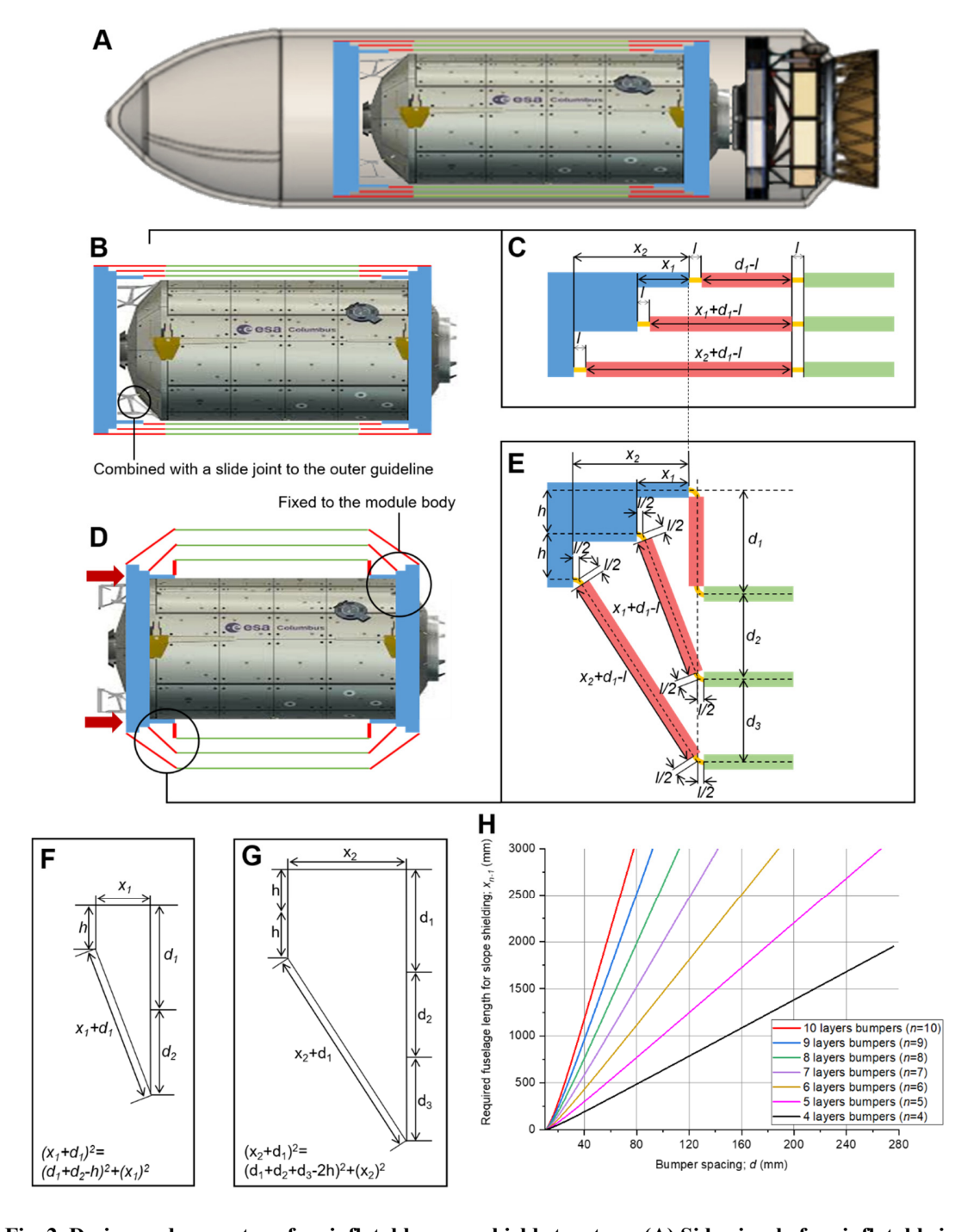


Fig. 2 Design and geometry of an inflatable space shield structure. (A) Side view before inflatable in rocket payload. (B) Side view before inflatable. (C) Geometry analysis before inflatable. (D) Side view after inflatable. (E) Geometry analysis after inflatable. (F) Habitation module without inflatable space shield structure. (G) Geometry analysis of the second bumper. (H) Graph of bumper spacing and number.

2) Pattern transition from paper model to prototype: The variable wheel design proposed in our previous study needed to be simplified. Since the payload has a straight fuselage, the rim part must be straight, and the excessively complex geometric transformation of the spoke part and many folds require a lot of energy to deploy, and

simplification for the purpose of the bumper was required. The straightened and simplified design graphics are shown in Figures 3 (C) and (D). Figures 3 (E-I), show a Z-shaped folded shape to fill the rim gap after expansion. Z-shaped folding is proposed for minimal diametrical space usage. However, through kinematic motion analysis, it was confirmed that if the bumpers were attached with almost no gap, geometric collisions occurred. The proposed design was actually implemented through the paper model (Fig.3 (K)). The corner of the folded part on the inclined shield side and the folded part of the rim part overlapped each other, resulting in a geometric collision. This conflict could be resolved by reducing the area of the Z-fold, but a gap was created.

Figure 2 (L) shows the actual implementation of the model with Kevlar/PE/epoxy. As the folding area of PE/epoxy composites widened, a lot of strain energy was required to realize excessive folding. In outer space, it is necessary to deploy using small-capacity actuators or small energy such as shape memory. It was judged that the proposed Z-fold design would be difficult to apply in space. Moreover, in the process of curing the composite, an additional composite sheet is required to bond the different faces together in the exploded view shown in Figure 3 (J), which leads to an increase in weight, and curing the composite in a non-planar 3D shape is very difficult. Therefore, a new design proposal was needed to consider all of the geometric collision, deformation energy accumulation, and ease of actual fabrication.

3) Final pattern: It is known from our previous studies that more flexible structures with no constraints can absorb more energy in ultra-velocity impacts. Also, there is almost no load on the shield in outer space. Therefore, the multi-shock shield deployed in outer space does not need to be reinforced with a high-strength structure. A new design inspired by that background and extendable steamer was proposed. Through much trial and error, the expansion structure in Figures 4 (D-H) was chosen, and it graphically shows a front-inflatable multi-shield structure to accommodate the thickness, taking into account both geometric and physical properties.

Before unfolding, if K1 is collinear with K2 on the y-axis, a collision occurs or a bending is required. Similarly, the collision of K3 and K4 and the collision of K5 and K6 can result in bending (Fig. 4 (H)). This discrepancy could be solved by placing a clear as much as the thickness of the bumper joint. In other words, K1 is located on the y-axis line with a higher thickness than K2. The positions of K3 and K5 have been adjusted in the same way. As the expansion diameter of the bumper increased, the width of the bumper extension (K6) also had to increase. The length of K6 must not exceed K5. Therefore, the expansion diameter (*d*) of the bumper is limited. Calculating the extension (*w*) of the bumper from the geometry of Figure 4 (H),

$$w = (r + d) \sin(22.5^{\circ}) - r \cdot \tan(11.25^{\circ}) \cdot \sin(67.5^{\circ}) - r \cdot \tan(11.25^{\circ}) = 0.3827 \cdot d - 10^{-14} \cdot r$$
 (8)

The coefficient of r is very small, so it can be approximated as:

$$w \approx 0.3827 \cdot d \tag{9}$$

Since w must be less than the width of the rim bumper,

$$0.3827 \cdot d < 2r \cdot \tan\left(11.25^{\circ}\right) \tag{10}$$

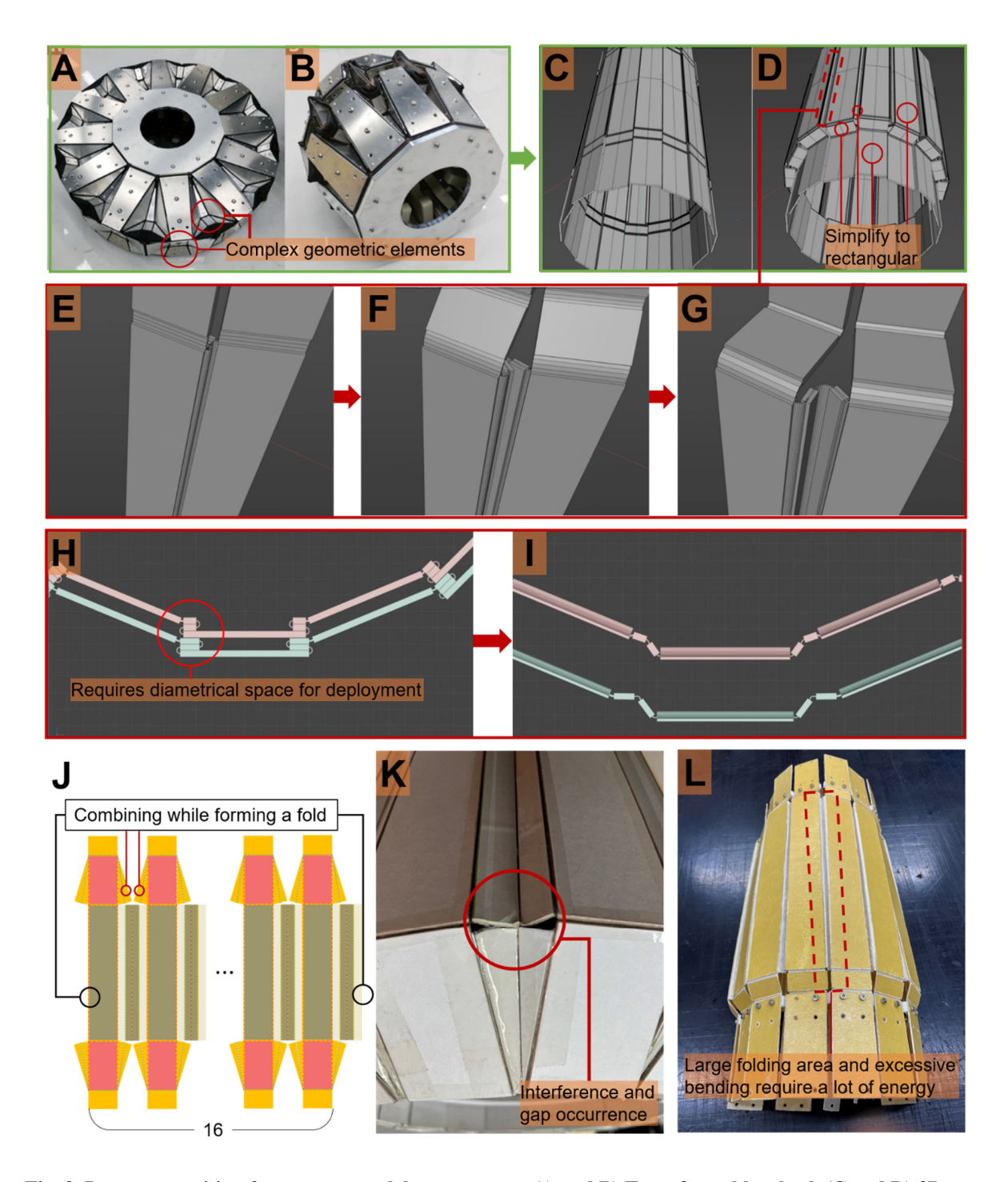


Fig. 3 Pattern transition from paper model to prototype. (A and B) Transformable wheel. (C and D) 3D modeling of simplified origami structures. (E, F and G) 3D modeling of the unfolding process of origami structures. (H and I) 3D modeling of the unfolding process of origami structures (front view). (J) Pattern. (K) Paper model. (L) Kevlar/PE/epoxy prototype model.

Simplifying the expression,

$$d < 1.04 \cdot r \tag{11}$$

This result means that the gap can be closed with the extended bumper only if the maximum inflation length is less than about 2.04r.

A model fabricated from real composites (Nextel/PE/epoxy and Kevlar/PE/epoxy) is shown in Figure 5.

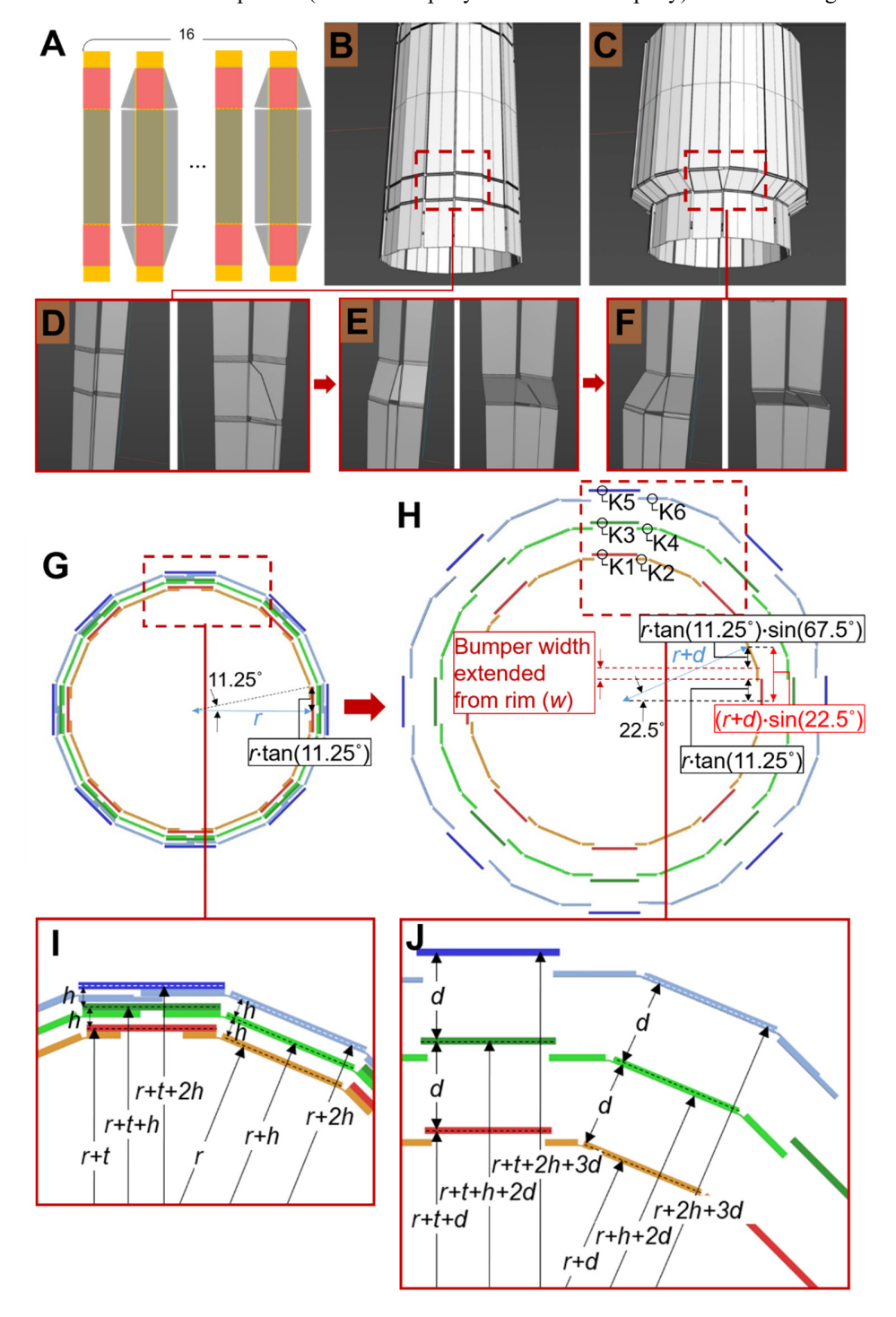


Fig. 4 Final pattern of the IMSS: (A) Pattern. (B and C) 3D modeling of simplified origami structures. (D, E and F) 3D modeling of the unfolding process of origami structures. (G, H, I, and J) 3D modeling of the unfolding process of origami structures (front view).

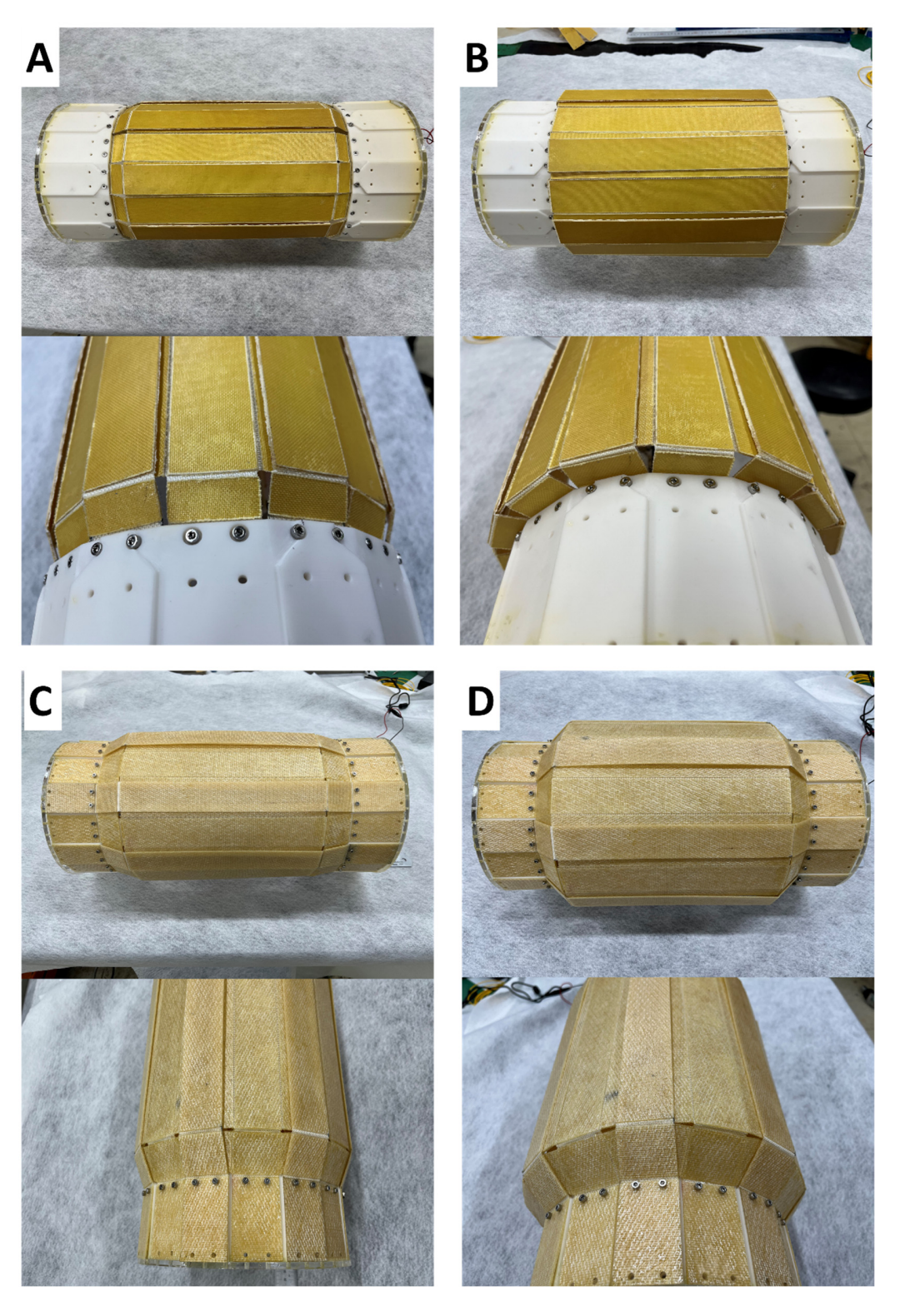


Fig. 5 IMSS implementation: (A) Before deployment of 1st bumper Kevlar/PE/epoxy. (B) After deployment of 1st bumper Kevlar/PE/epoxy. (C) Before deployment of 2st bumper Nextel/PE/epoxy. (D) After deployment of 2st bumper Nextel/PE/epoxy.

B. Hypervelocity impact of origami shield composites

Fig. 6 (A) shows the hypervelocity impact equipment owned by the Department of Aerospace Engineering at KAIST. Fig. 6 (B) shows the specimen contained inside the impact chamber. Fig. 6 (C) is a schematic diagram of a hypervelocity impact. By measuring the initial velocity (v_i) and penetration velocity (v_f) , the projectile's kinetic energy reduction rate can be calculated. Fig. 6 (D) is a picture taken from the side of the specimen after a hypervelocity impact. Fig. 6 (E) is the experimental result when the bumper gap is 0 mm. Fig. 6 (F) is the experimental result when the bumper gap is 14 mm. From the experimental results, it can be confirmed that the larger the bumper gap, the larger the fiber pull-out. Fig. 6 (G) shows the change in impact energy according to the bumper spacing. From the experimental results, it can be confirmed that the bulletproof performance can be maximized when the bumper gap is up to 20 mm (Fig. 6 (G)).

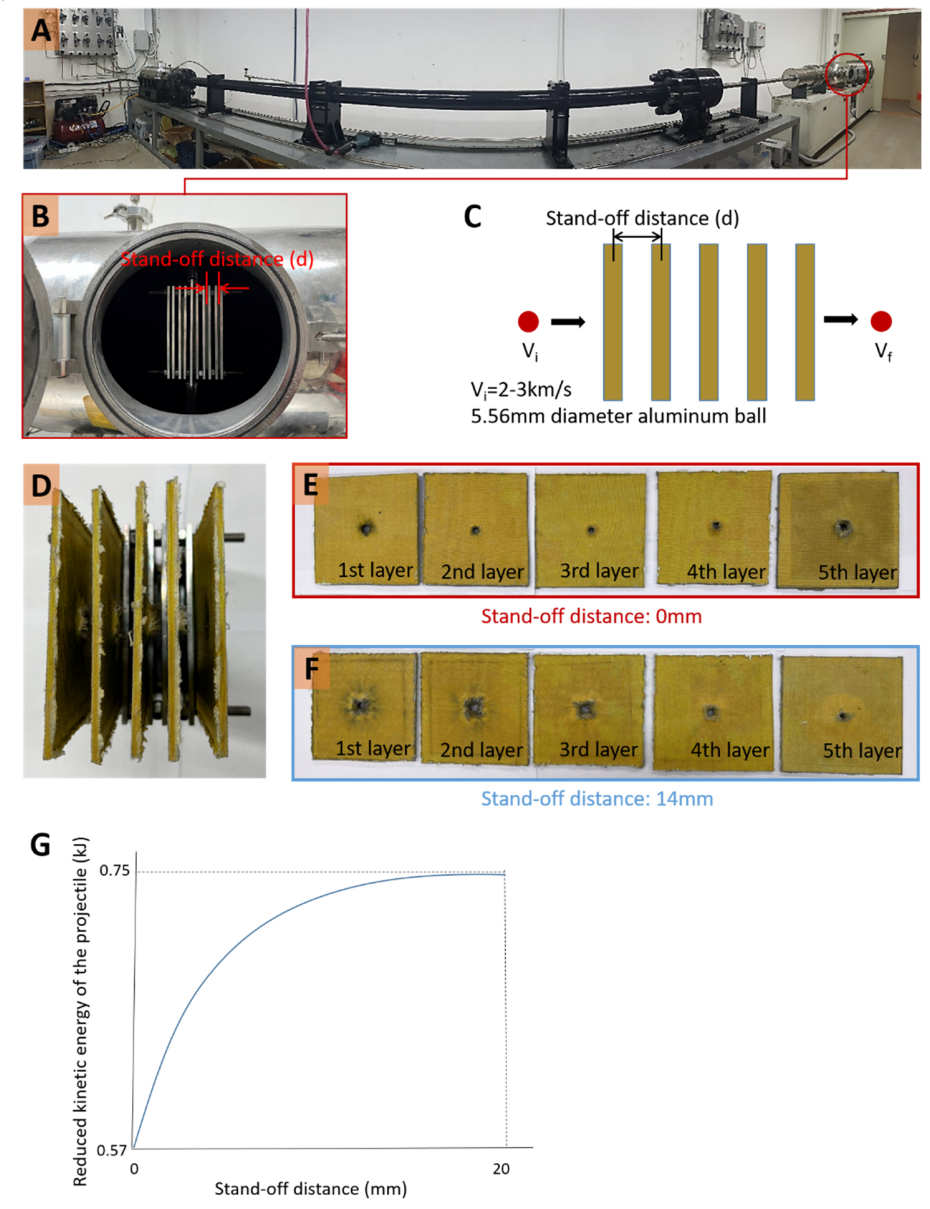


Fig. 6 Hypervelocity impact test. (A) Hypervelocity impact equipment (two-stage light gas gun). (B) Specimens with stand-off distance set. (C) Schematic diagram of hypervelocity impact test. (D) Specimens after hypervelocity impact (2.0-2.1 km/s). (E) Specimens with a stand-off distance of 0 mm after hypervelocity impact (2.0-2.1 km/s). (F) Specimens with a stand-off distance of 14 mm after hypervelocity impact (2.0-2.1 km/s). (G) Reduced kinetic energy of the projectile according to stand-off distance.

C. Space environment resistance of origami shield composites

In Fig. 7 (A), the proposed space shield-origami composite structure is shown. This structure is made of PE/epoxy composites material. Fig. 7 (B) is the geometrical analysis of the folding tolerance. Fig. 7 (C) is space environment simulation equipment set to simulate the lunar orbit. Fig. 7 (D) shows a specimen prepared for space environment testing. Fig. 2 (E) shows the total mass loss (TML) rate according to the period in the space environment test simulating the lunar orbit environment.

Since the TML is lower than 1.0% even in the worst-case folding state without tolerance, it can be determined that it is applicable to the space environment (Fig. 2 (E)). As the folding tolerance increases, the TML decreases, but the TML is higher than that of CFRP (Fig. 2 (E)).

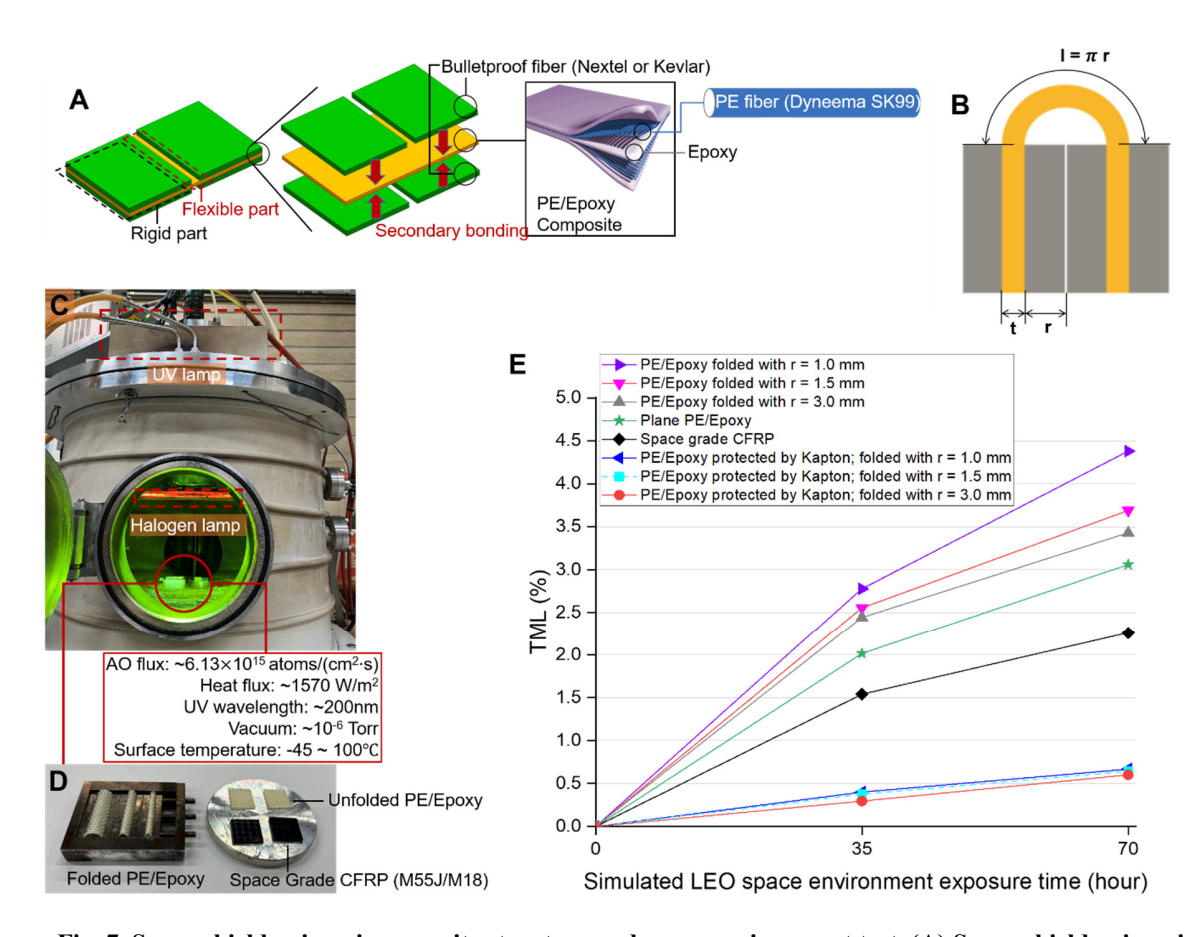


Fig. 7 Space shield-origami composite structure and space environment test. (A) Space shield-origami composite structure. (B) Folded to suitable tolerance. (C) Space environment simulation test equipment. (D) Specimens in the space environment chamber. (E) TML test results according to space environment exposure time.

IV. Conclusion

The Whipple shield is used in spacecraft as an outer wall structure to protect against micrometeoroids. By increasing the stand-off distance of the Whipple shield and using a multi-layered shield structure, it is possible to increase bulletproof performance against micrometeoroids. Due to payload diameter limitations, the Whipple shield's stand-off distance cannot be significantly increased. Increasing the stand-off distance of the Whipple shield reduces the volume inside the spacecraft. To solve this problem, an origami structure in which a multilayer shield expands in a radial direction has been proposed. PE/Epoxy composites have been proposed to realize origami structures. When the PE/Epoxy composites were bent, the resistance to the low-Earth orbit space environment was evaluated and

compared with that of the plane PE/Epoxy composites. In order to increase the resistance to the space environment, a method of secondary curing of Kapton and bulletproof fibers together in the flexible part has been proposed. Hypervelocity impact tests were conducted to improve and verify the performance of the proposed inflatable structure. The radiant heat shielding performance of the proposed multilayer structure of ceramic fibers and flexible composites and multi-layer insulation (MLI) was compared, and it was confirmed that the radiant heat shielding performance was comparable to that of MLI. The geometry of the proposed inflatable origami structure was analyzed and the folding pattern was determined. The proposed inflatable origami structure confirmed the diameter reduction effect and improved bulletproof performance compared to the conventional Whipple shielding structure.

Copyright Statement

The authors confirm that they, and/or their company or organization, hold copyright on all of the original material included in this paper. The authors also confirm that they have obtained permission, from the copyright holder of any third party material included in this paper, to publish it as part of their paper. The authors confirm that they give permission, or have obtained permission from the copyright holder of this paper, for the publication and distribution of this paper as part of the ICAS proceedings or as individual off-prints from the proceedings.

References

- [1] C.Zeitlinet al., Measurements of Energetic Particle Radiation in Transit to Mars on the Mars Science Laboratory, Science (2013).
- [2] Zhang S, Wimmer-Schweingruber RF, Yu J, Wang C, Fu Q, Zou Y, et al. (2020). "First measurements of the radiation dose on the lunar surface". Science Advances. 6 (39).
- [3] Boyle, Rebecca. "The moon has hundreds more craters than we thought". Archived from the original on 13 October 2016.
- [4] Gonzalo, Jesús, Domínguez, Diego, López, Deibi. "On the challenge of a century lifespan satellite." Progress in Aerospace Sciences vol. 70 (2014): 28-41.
- [5] Mighani, S.; Wang, H.; Shuster, D.L.; Borlina, C.S.; Nichols, C.I.O.; Weiss, B.P. (2020). "The end of the lunar dynamo". Science Advances.
- [6] "Earth's Moon Hit by Surprising Number of Meteoroids". NASA. 13 October 2016. Archived from the original on 2 July 2022. Retrieved 21 May 2021.
- [7] Hartmann, William K.; Quantin, Cathy; Mangold, Nicolas (2007). "Possible long-term decline in impact rates: 2. Lunar impact-melt data regarding impact history". Icarus. 186 (1): 11–23.
- [8] Lyndon B. Johnson Space Center Houston, Handbook for Designing MMOD Protection, NASA Johnson Space Center (2009).
- [9] Origami transformable wheel Dae-Young Lee et al., High-load capacity origami transformable wheel, SCIENCE ROBOTICS (2021).
- [10] D. Iguchi et al., Development of hydrogen-rich benzoxazine resins with low polymerization temperature for space radiation shielding, ACS Omega, 3 (2018).
- [11] Miura-origami core Jianjun Zhang et al., A study on ballistic performance of origami sandwich panels, International Journal of Impact Engineering (2021).
- [12] Singleterry RC et al., OLTARIS: On-line tool for the assessment of radiation in space. Acta Astronaut, (2011).